

KLF4 suppresses the proliferation of perihilar cholangiocarcinoma by negatively regulating GDF15 and phosphorylating AKT

XIAOMING ZHANG, WEIJIA WANG, CHUNLEI LU and HAIFENG ZHANG

General Surgery Center of Linyi People's Hospital, Linyi, Shandong 276000, P.R. China

Received October 30, 2022; Accepted June 7, 2023

DOI: 10.3892/or.2023.8659

Abstract. Krüppel-like factor 4 (KLF4) is a transcription factor which functions as a tumor suppressor or an oncogene in numerous types of solid tumors. However, its expression levels and function in perihilar cholangiocarcinoma (pCCA) have yet to be elucidated. In the present study, in order to investigate its roles in pCCA, reverse transcription-quantitative PCR (RT-qPCR), western blot analysis and immunohistochemistry were used to detect KLF4 expression in pCCA. The Chi-squared test was used to analyze the associations between KLF4 and the clinicopathological features of patients with pCCA. Univariate and multivariate analyses were subsequently used to analyze the prognostic significance of KLF4. The tumor suppression of KLF4 was investigated for the purposes of illustrating its biological function both *in vitro* and *in vivo*. Furthermore, the association between KLF4 and growth/differentiation factor 15 (GDF15) was determined using pCCA tissue microarray (TMA) analysis and RT-qPCR. The underlying molecular mechanisms between KLF4 and GDF15 were subsequently investigated *in vitro*. In pCCA tissues, KLF4 was found to be downregulated, and this was negatively associated with the histological grade and tumor size. The knockdown of KLF4 was also found to be a prognostic indicator of the poorer survival of patients with pCCA. Based on *in vitro* and *in vivo* analyses, KLF4 was found to suppress tumor progression and induce cell apoptosis. Furthermore, it was found that KLF4 executed its tumor suppressive effects via the regulation of the GDF15/AKT signaling pathway. Taken together, the findings of the present study demonstrate that KLF4 may be considered as an independent biomarker of a favorable prognosis of patients with pCCA, and the KLF4/GDF15/AKT signaling

pathway may potentially be a novel molecular therapeutic target for patients with pCCA.

Introduction

Cholangiocarcinoma (CCA) is an epithelial cell malignancy that originates from cholangiocytes, and which can occur at any level of the biliary tree (1). The overall incidence of CCA has been increasing worldwide over the course of the last few decades (1-3). CCAs are usually symptomless in the early stages of the disease; therefore, they are often not diagnosed until the disease has progressed to an advanced stage, which severely compromises the therapeutic options available, resulting in an unfavorable prognosis (2). Anatomically, CCAs can be classified into three groups as follows: Intrahepatic, perihilar and distal (4). Perihilar CCA (pCCA) is the most common subtype of CCA, representing ~50-60% of all cases of CCA; ~30-40% of cases are distal carcinomas, whereas intrahepatic carcinomas represent <10% of CCA cases (5,6). Surgical resection has been the mainstay of curative treatment for the three subtypes of CCA. However, patients with pCCA are not able to receive the full benefits of surgical resection due to the difficulty of early detection, vascular invasion and lymphatic metastasis in the advanced stages of the disease (7). Although significant progress has been made with chemotherapeutics, targeted therapy and immunotherapy as alternative treatments, to date, these therapies have not demonstrated any notable benefits in terms of the overall survival (OS) rates of patients with pCCA (1). Therefore, there is an urgent need for the identification of novel biomarkers and drug targets for improving the diagnosis and treatment of patients with pCCA.

Krüppel-like factor 4 (KLF4) is a zinc finger-containing transcription factor that is able to regulate diverse cellular processes, including cell growth, proliferation and differentiation (8). It is predominantly expressed in terminally differentiated epithelial tissues, such as the skin, lungs and the gastrointestinal tract (9). However, a variety of studies have demonstrated that KLF4 functions via diverse and even opposite mechanisms in various types of tumors. For example, KLF4 is downregulated in a number of types of epithelial cancer, including esophageal, gastric, colorectal and bladder cancer (10-13), leading to cell proliferation. On the other hand, conflicting results have demonstrated that KLF4 is overexpressed in primary breast and prostate cancer (14,15), where it

Correspondence to: Professor Chunlei Lu or Dr Haifeng Zhang, General Surgery Center of Linyi People's Hospital, The Intersection of Wohushan Road and Wuhan Road, Linyi, Shandong 276000, P.R. China

E-mail: juanmeiforever@163.com

E-mail: 2017120371@mail.sdu.edu.cn

Key words: Krüppel-like factor 4, perihilar cholangiocarcinoma, prognosis, proliferation, growth/differentiation factor 15

plays an oncogenic role in tumor development and progression. However, the underlying mechanisms through which KLF4 exerts its functions in pCCA, and its prognosis value, have yet to be fully elucidated.

Growth and differentiation factor 15 (GDF15) is a divergent member of the TGF- β superfamily. Over the course of the past few years, it has been shown to participate in carcinogenesis and tumor progression. Previous studies have indicated that GDF15 expression is elevated in certain types of tumor, including non-small cell lung cancer (16), cervical cancer (17), liver cancer (18), head and neck cancer (19), esophageal cancer (20), and so on (21-24). However, certain studies have suggested that GDF15 may have a tumor-suppressive activity in various types of cancer cells, or at different stages of tumor growth (25). GDF15 has been shown to function as a tumor activator or suppressor through the Smad, AKT and ERK signaling pathways (26). However, to date, the biological functions of GDF15 in pCCA remain unclear.

KLF4 and KLF5, the closest members of the KLF family, fulfill key roles in tumor proliferation, differentiation and carcinogenesis in esophageal cancer and gastrointestinal carcinoma (27,28). Zhao *et al* (16) reported that GDF15, as the downstream target of KLF5, was able to increase the rate of tumor cell proliferation. However, the association between KLF4 and GDF15 in pCCA has yet to be elucidated.

In the present study, it was demonstrated that KLF4 was a favorable prognostic factor in pCCA. It has been shown to inhibit the proliferation and promote the apoptosis of cholangiocarcinoma cells. The findings presented herein also demonstrate that KLF4 suppression enhances the transcription of GDF15 in pCCA, suggesting that the KLF4/GDF15 signaling axis may be a potential therapeutic target in pCCA.

Materials and methods

Patients and follow-up. The present primary study cohort comprised 242 patients who were diagnosed with pCCA at Linyi People's Hospital (Linyi, China), and who underwent surgical resection from 2010 to 2020. A validation cohort contained 114 patients who were selected from the primary cohort according to the following inclusion criteria: i) Patients who underwent radical resection with a clear surgical margin; ii) patients with available formalin-fixed tumor tissues, follow-up information and complete medical records; iii) patients with a post-surgical survival time of >1 month; and iv) patients with no history of other malignancies. The primary end point of follow-up was the OS rate (note that determination of the OS rate excluded deaths that may have resulted from any other cause besides cancer-specific death).

Clinical tissue samples. A total of 20 paired tumor specimens and adjacent normal tissues were obtained from patients with pathologically verified pCCA who received R0 surgery at Linyi People Hospital. The present study was approved by the Medical Ethics Committee of Linyi People's Hospital (approval no. YX200626). Written informed consent was obtained from each patient prior to inclusion in the study.

Tissue microarray (TMA) and immunohistochemistry (IHC). A pCCA TMA containing the aforementioned 114 specimens was immunohistochemically stained for KLF4 (cat. no. ab215036; Abcam) and GDF15 (cat. no. ab206414; Abcam). The TMA slides were submerged in EDTA (pH 9.0) buffer for optimal antigen retrieval. Primary KLF4 antibody (1:500) or GDF15 antibody (1:100) was applied and incubated with the specimens at 4°C overnight. A biotin-labeled goat anti-rabbit antibody (OriGene Technologies, Inc.; formerly ZSGB/ZSGB-BIO) was applied to the specimens for 30 min at room temperature. Subsequently, the slides were incubated with conjugated horseradish peroxidase-streptavidin. The peroxidase reaction was developed using 3,3'-diaminobenzidine (DAB) solution (OriGene Technologies, Inc.). The stained TMA was subsequently scanned using a HistoRX PM-2000 (TM) imaging system and analyzed using AQU Analysis software (version 2.3.3.2, HistoRx, Inc.), which was used to generate the IHC scores. The IHC scores were calculated according to the following formula: IHC score=(percentage of cells with weak staining intensity x1) + (percentage of cells with moderate staining intensity x2) + percentage of cells with strong staining intensity x3). The cohort of specimens was divided into two subgroups, according to the cut-off value of KLF4 scores, which were identified as the point with the highest sum of specificity and sensitivity in the receiver operating characteristic (ROC) curve. The cut-off value for KLF4 in pCCA was identified to be 71.2. The scores of KLF4 and GDF15 of the TMA were analyzed to find the associated correlation values using Spearman's correlation analysis.

Cell lines and cell culture. The human pCCA cell lines, QBC939 (cat. no. CC-Y1636) and FRH0201 (cat. no. YS1612C), the intrahepatic cholangiocarcinoma (IHCC) cell line RBE (cat. no. HTX1698), and the biliary epithelial cell line [human intrahepatic biliary epithelial cells (HIBEpIC; cat. no. YS2223C)] were obtained from the Cell Bank of Shanghai Yaji Biotechnology Co., Ltd. The QBC939 and HIBEpIC cell lines were maintained in Gibco® DMEM (Thermo Fisher Scientific, Inc.), containing 10% Gibco® fetal bovine serum (FBS; Thermo Fisher Scientific, Inc.) and 100 U/ml Gibco® penicillin/streptomycin (Thermo Fisher Scientific, Inc.). The RBE and FRH-0201 were cells maintained in Gibco® RPMI-1640 medium (Thermo Fisher Scientific, Inc.) supplemented with 10% Gibco® FBS and 100 U/ml Gibco® penicillin/streptomycin (Thermo Fisher Scientific, Inc.). All the cell lines were cultured at 37°C in a humidified incubator containing 5% CO₂.

Transient transfection and lentiviral transduction. A KLF4 overexpression plasmid and negative control vector, KLF4-specific shRNA and non-coding shRNA were synthesized by GenePharma. GDF15 siRNAs were purchased from GeneChem, Inc. The sequence of the siRNA targeting GDF15 was as follows: 5'-GCTACAATCCCATGGTGCTCA-3'. The sequence of the control siRNA was as follows: 5'-UUCUCCGAACGUGUCACGUTT-3'. For transient transfection, the cells were seeded in six-well plates at a density of 4x10⁵ cells/well. Upon reaching 70% confluency, the cells were transfected with the siRNAs or plasmids. siRNA (100 pmol) or plasmids (4 μ g) were transfected into the cells

using Lipofectamine 2000 reagent (GenePharma Co., Ltd.) at 37°C for 8 h, according to the manufacturer's protocol. At 8 h post-transfection, the cell culture medium was discarded, and fresh DMEM containing 10% v/v FBS was added to each well. After 48 h, the transfection efficiency was further assessed using western blot analysis and subsequent experimentations were executed. For lentiviral transduction, the 2nd generation system was used in the lentivirus transduction experiment. MOI values and optimal infection conditions were determined by pre-testing. The cells were seeded in six-well plates at a density of 3×10^5 cells/well. Upon reaching 30% confluency, the cells were transfected with the shRNAs. The shRNAs (MOI, 60) were transduced into cells (GenePharma Co., Ltd.) at 37°C for 16 h, according to the manufacturer's protocol. The cell culture medium was then discarded, and fresh DMEM containing 10% v/v FBS was added into each well. After 72 h, the transduction efficiency was observed using a fluorescence microscope (Olympus Corporation). Stable cell lines with KLF4 knockdown were selected using 4 μ g/ml puromycin for 7 days. Western blot analysis was conducted to detect the knockdown efficiency of *KLF4*.

RNA extraction and reverse transcription-quantitative PCR (RT-qPCR). Total RNA was extracted from the pCCA cultured cells, tumor tissues and adjacent normal tissues using Invitrogen™ TRIzol™ reagent (Thermo Fisher Scientific, Inc.). Subsequently, the total RNA was reverse transcribed to obtain first-strand cDNA using an RNA-PCR kit (cat. no. FSQ-101; Toyobo Life Science), following the manufacturer's protocols. The resulting cDNA was used for RT-qPCR using an Applied Biosystems® SYBR-Green PCR Master Mix kit (cat. no. A25742; Thermo Fisher Scientific, Inc.). The thermocycling conditions were as follows: Pre-denaturation at 93°C for 2 min; 40 cycles of denaturation at 93°C for 1 min; annealing at 55°C for 1 min; extension at 72°C for 1 min; and final extension at 72°C for 7 min. Quantification of the relative mRNA levels was normalized against that of GAPDH and calculated using the $2^{-\Delta\Delta C_q}$ method (29). The primers used were as follows: *KLF4* forward, 5'-CTGCGAACCCACACAGGTAG-3' and reverse, 5'-TGGAAGCTAACCTGGGAAGTC-3'; and *GDF15* forward, 5'-ACTCACGCCAGAAGTGCG-3' and reverse, 5'-CACGTCCCACGACCTTGAC-3'; and *GAPDH* forward, 5'-GAAAGCCTGCCGGTGACTAA-3' and reverse, 5'-GCCCAATACGACCAATCAGAG-3'.

Western blot analysis. Cell lysates and tissues were lysed using RIPA lysis buffer (Beyotime, Institute of Biotechnology), and the total protein concentration was determined using a BCA protein detection kit (Pierce; Thermo Fisher Scientific, Inc.). Target proteins (30 μ g/lane) were separated by SDS-PAGE (8-15% gels) and then blotted onto polyvinylidene fluoride (PVDF) membranes. After blocking the membranes with 5% bovine serum albumin at room temperature for 1 h, the PVDF membranes were incubated with primary antibodies at 4°C overnight. The following antibodies were used: Anti-KLF4 (1:1,000; cat. no. ab215036; Abcam); anti-GDF15 (1:1,000; cat. no. ab206414; Abcam); anti-Lamin B (1:1,000; cat. no. AF1408; Beyotime Institute of Biotechnology); anti-GAPDH (1:1,000; cat. no. AF1186; Beyotime Institute

of Biotechnology); anti-Bcl-2 (1:1,000; cat. no. ab32124; Abcam); anti-Bax (1:1,000; cat. no. ab32503; Abcam); anti-AKT (1:500; cat. no. 4691; Cell Signaling Technology, Inc.); and anti-phosphorylated (p-)AKT (1:500; cat. no. 4060; Cell Signaling Technology, Inc.). Subsequently, the membranes were incubated with secondary antibodies (HRP-linked goat anti-rabbit IgG antibodies; 1:500; cat. no. A0208; Beyotime Institute of Biotechnology) for 1 h at room temperature. Proteins were visualized using enhanced chemiluminescence detection (Beijing Solarbio Science & Technology Co., Ltd.). Protein bands were quantified using ImageJ software (v 1.46r, National Institutes of Health) if necessary.

Cell proliferation assay. Cell proliferation was detected using Cell Counting Kit-8 (CCK-8) and 5-ethynyl-2'-deoxyuridine (EdU) assays. The transfected cells were seeded in 96-well plates at a density of 3×10^3 cells per well, and incubated at 37°C for time periods of 24, 48, 72 and 96 h. Every 24 h, the cells were mixed with 10 μ l CCK-8 reagent (Dojindo Laboratories, Inc.) per well, and subsequently incubated further with the CCK-8 reagent at 37°C for 1 h. The absorbance value at 450 nm was then measured using a microplate reader (Thermo Fisher Scientific, Inc.). The relative OD₄₅₀ values were calculated using the formula: OD₄₅₀ of the tested well-OD₄₅₀ of the empty medium.

The fraction of DNA-replicating cells, which represents the cell proliferation status, was assessed using an EdU detection kit (Guangzhou RiboBio Co., Ltd.), in accordance with the manufacturer's protocol. Briefly, the FRH0201 and QBC939 cells were cultured in 96-well plates at 6×10^3 cells per well, and incubated at 37°C for 24 h. Subsequently, 50 μ M EdU labeling medium was added to the 96-well plates and the cells were incubated at 37°C for 2 h. The cells were then treated with 4% paraformaldehyde and 0.5% Triton X-100. The cells were stained with Apollo reaction mixture at 37°C for 30 min. Hoechst 33342 was used to label cell nuclei at 37°C for 30 min. The EdU incorporation rate was calculated as the ratio of the number of EdU-incorporated cells to the number of Hoechst 33342-stained cells. At least 500 cells were counted for every group.

Apoptosis detection. Cell apoptosis was detected using a PE-Annexin V Apoptosis Detection Kit (BD Biosciences). Cells contained in the supernatant were harvested by centrifugation at 500 x g for 5 min at 4°C. The cells were then washed with PBS and resuspended in a binding buffer containing PE-Annexin and 7-aminoactinomycin D (7-AAD), following the manufacturer's instructions. After the cells were incubated for 15 min at 25°C in the dark, the percentages of apoptotic cells were analyzed using a flow cytometer (FACSCanto II, BD Biosciences).

A terminal deoxynucleotidyl transferase (TdT)-mediated dUTP nick-end labeling (TUNEL) assay was also used to assess cell apoptosis. The transfected cells were seeded in 30-mm Petri dishes and cultivated to a confluency of not >80% per Petri dish. Cell fixation, permeabilization and TdT incubation were performed following the manufacturer's instructions provided with the TUNEL Apoptosis Detection kit (Alexa Fluor 647; Shanghai Yeasen Biotechnology Co., Ltd.).

In vivo tumorigenicity assays. All animal experiments were approved by the Medical Ethics Committee of Linyi People's Hospital. They were executed in accordance with the guidelines for the use and care of laboratory animals provided by Linyi People's Hospital. Female BALB/c nude mice (6–8 weeks of age; weighing 20–24 g; n=12, 6 mice/cage) were purchased from GenePharm Biotech Corp and housed in a specific pathogen-free environment (at 25°C, 60% relative humidity and 12-h light/dark cycle). The mice were provided with food and water *ad libitum* in the animal research center. The mice were randomly divided into two groups, each containing 6 mice. The FRH0201 cells (4×10^6) transfected with shKLF4 or a negative control (NC) were subcutaneously injected into the right flanks of the mice. Tumor diameters were measured every 3 days, and the tumor volumes were calculated using the following formula: $V = \text{length} \times \text{width}^2 / 2$ (mm^3). The mice were sacrificed by cervical dislocation following an intraperitoneal injection of pentobarbital on the 21st day, and the xenograft tumors were removed, weighed and photographed (the maximum tumor volume permitted in our study was $< 2,000 \text{ mm}^3$).

Bioinformatics analyses. The microarray expression data of GSE26566 and GSE89749 were obtained from the Gene Expression Omnibus database (GEO). The dataset GSE26566 based on the platform of GPL6104 platform (Illumina humanRef-8 v2.0 expression beadchip) including 104 cholangiocarcinoma tumor samples and 6 normal bile duct samples. The dataset GSE89749 based on the platform of GPL10558 platform (Illumina HumanHT-12 V4.0 expression beadchip) containing 118 cholangiocarcinoma tumor samples and 2 normal bile duct samples. To screen the differentially expressed genes (DEGs) between the cholangiocarcinoma tumor samples and normal bile duct samples, we used the GEO2R online web tool, which allows users to compare different gene expression data of two or more groups of samples. An adjusted P-value < 0.05 and $\log_2(\text{FC}) \geq 1.5$ were set as the thresholds for identifying DEGs. DEGs with $\log_2(\text{FC}) > 0$ were considered as upregulated genes, and those with $\log_2(\text{FC}) < 0$ were classified as downregulated genes. To identify the intersectional genes between GSE26566 and GSE89249, the Venny 2.1 online web tool was used to create a Venn diagram.

Statistical analysis. Statistical analyses were performed using SPSS17.0 (SPSS, Inc.) and GraphPad Prism 6.0 (Dotmatics) software packages. Data are expressed as the mean \pm standard deviation (SD). All experiments were repeated three times unless otherwise specified. The associations between KLF4 and the clinicopathological characteristics of patients with pCCA were analyzed using the Chi-squared (χ^2) test. Univariate and multivariate Cox regression analyses were used for the survival data. The correlation between KLF4 and GDF15 was determined using Spearman's correlation analysis for IHC Scores. Pearson's correlation analysis was used for the data obtained from RT-qPCR. A paired or unpaired t-test was used to compare differences between two groups, whereas one-way ANOVA was used to analyze the differences among three groups. If there were significant differences, multiple comparisons were made between the groups (using Tukey's test). $P < 0.05$ was considered to indicate a statistically significant difference.

Results

KLF4 expression levels in pCCA and adjacent tissues. To determine the expression of KLF4 in pCCA, the expression level of KLF4 was first detected in 20 pairs of pCCA tissues and adjacent normal bile duct tissues using RT-qPCR analysis (Fig. 1A). Compared with the expression level in normal tissues, KLF4 mRNA expression was found to decrease in the majority of pCCA tissues. KLF4 protein levels in four pairs of these pCCA tissues were subsequently detected using western blot analysis, and these experiments revealed that the expression level of KLF4 protein and the corresponding mRNA was decreased in pCCA (Fig. 1B). Furthermore, KLF4 expression was analyzed in human pCCA TMAs; two representative images of KLF4 expression (high and low or positive/negative) obtained from TMAs are presented in Fig. 1C. As a transcription factor, KLF4 was shown to be located in the nucleoplasm and cytosol.

Association between KLF4 and the pathological features of patients with pCCA. To further determine the level of KLF4 expression, and to examine the association between KLF4 and the clinical features of patients with pCCA, pCCA TMAs containing 114 cases of pCCA were used for IHC. The clinicopathological features of the patients with pCCA in the TMAs were recorded and analyzed. Cox survival analysis revealed that a high level of KLF4 expression was a marker of a favorable prognosis for patients with pCCA ($P < 0.001$, Fig. 1D). Subsequently, the associations between KLF4 and the clinicopathological factors of patients with pCCA were analyzed. Notably, as shown in Table I, KLF4 expression was found to be negatively associated with histological grade ($P = 0.004$) and tumor size ($P = 0.022$). However, KLF4 expression was not found to be associated with age, sex, tumor depth, lymphatic metastasis and tumor lymph node-metastasis (TNM) stage (all $P > 0.05$; Table I). Subsequently, a Cox proportional hazards model was performed in order to better determine whether KLF4 expression should be regarded as a valuable biomarker (Table II). Univariate analysis revealed that histological grade ($P = 0.001$), tumor size ($P = 0.024$), TNM stage ($P = 0.003$) and KLF4 expression ($P = 0.002$) were significantly associated with the risk of mortality. Further multivariate analyses were performed to identify the aforementioned factors, and the outcomes confirmed that KLF4 expression ($P = 0.022$) was an independent prognostic indicator for OS in pCCA, as were histological grade ($P = 0.017$) and TNM stage ($P = 0.003$).

KLF4 suppresses pCCA cell proliferation in vitro. To examine the effects of an altered KLF4 expression on the proliferation of pCCA cells, the expression of KLF4 was detected in a series of cell lines, including the pCCA cell lines, QBC939 and FRH0201, the IHCC cell line, RBE, and the normal biliary epithelium cell line, HIBEpic, using RT-qPCR and western blot analyses. KLF4 was expressed at prominent levels in the FRH0201 and RBE cells, although its expression was only at a relatively low level in the QBC939 cells (Fig. 2A). Consequently, the QBC939 cells and FRH0201 cells were used for further functional analyses. The expression of KLF4 was knocked down in the FRH0201 cells, whereas KLF4

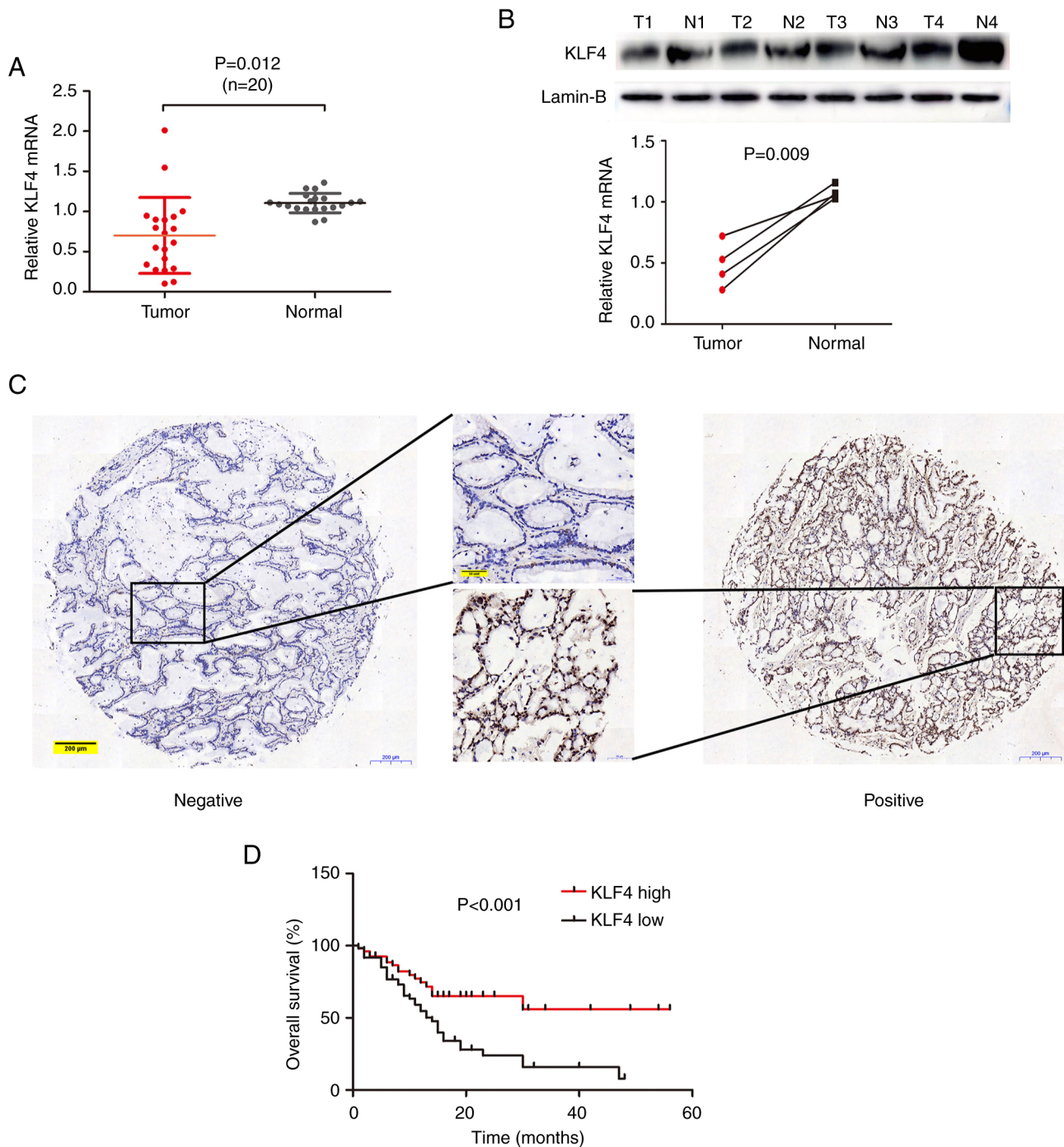


Figure 1. Expression levels of KLF4 in pCCA tissues and the association between the overall survival rates and clinicopathologic factors of patients with pCCA. (A) Relative mRNA levels of KLF4 in pCCA (n=20) tissues and adjacent normal tissues were detected using RT-qPCR. The results were analyzed using the $2^{-\Delta\Delta C_t}$ method, with GAPDH as a reference gene. Statistically significant differences between groups were assessed using a paired sample t-test. (B) The protein and mRNA expression levels of KLF4 were detected in four pairs of pCCA tissues and adjacent normal tissues using western blot analysis and RT-qPCR. Lamin B served as a loading control. 'N' represents 'Normal', whereas 'T' represents 'tumor' tissues. (C) Representative immunohistochemical images of KLF4 in human pCCA tissues are shown. (D) Patients with a high KLF4 expression had improved overall survival rates compared with those with a low KLF4 expression (P=0.002). KLF4, Krüppel-like factor 4; pCCA, perihilar cholangiocarcinoma; RT-qPCR, reverse transcription-quantitative PCR.

overexpression was induced in the QBC939 cells. As shown in Fig. 2B and C, the knockdown or overexpression efficiency was detected using RT-qPCR and western blot analyses. CCK-8 and EdU assays subsequently revealed that the knockdown of KLF4 expression promoted cell proliferation (Fig. 2D and F) in the shKLF4 group, whereas KLF4 overexpression led to a marked suppression of cell proliferation (Fig. 2E and G) in the KLF4 group compared with the control and NC groups. Taken

together, these results suggest that KLF4 plays an essential role in the proliferation of pCCA cells.

Knockdown of KLF4 expression suppresses apoptosis. The inhibition of apoptosis is also crucially involved in tumor development, in addition to the deregulated proliferation of cancer cells (30). Therefore, in the present study, flow cytometric analysis was performed to assess the percentage of

Table I. Associations between KLF4 expression and the clinicopathological characteristics of patients with pCCA.

Characteristic	No. of cases	KLF4 expression		χ^2 value	P-value
		High (n)	Low (n)		
Age (years)					
>63	60	25	35	1.652	0.199
≤63	54	29	25		
Sex					
Male	81	43	38	3.670	0.055
Female	33	11	22		
Histological grade					
Well and moderately differentiated	96	51	45	8.082	0.004
Poorly differentiated	18	3	15		
Tumor size (cm)					
>2.5	53	19	34	5.272	0.022
≤2.5	61	35	26		
Tumor depth					
T1	40	21	19	0.651	0.420
T2-T4	74	33	41		
Lymphatic metastasis					
Absent	75	32	43	41.944	0.163
Present	39	22	17		
TNM stage					
I and II	73	33	40	0.381	0.537
III and IV	41	21	20		

Values in bold font indicate statistically significant differences (P<0.05). KLF4, Krüppel like factor 4; pCCA, perihilar cholangiocarcinoma.

Table II. Univariate and multivariate analyses of prognostic factors for the overall survival of patients with pCCA.

Variable	Univariate analysis			Multivariate analysis ^a		
	HR	95% CI	P-value	HR	95% CI	P-value
Age, years (>63 vs. ≤63)	0.647	0.376-1.114	0.116			
Sex (male vs. female)	1.077	0.612-1.897	0.797			
Histological grade (well and moderately vs. poorly differentiated)	2.912	1.533-5.534	0.001	2.265	1.155-4.443	0.017
Tumor size (>2.5 vs. ≤2.5)	0.538	0.314-0.920	0.024			
Tumor depth (T1 vs. T2-4)	1.363	0.737-2.520	0.323			
Lymphatic metastasis (absent vs. present)	1.472	0.857-2.528	0.161			
TNM stage (I/II vs. III/IV)	2.227	1.310-3.784	0.003	2.305	1.341-3.962	0.003
KLF4 expression (high vs. low)	0.403	0.225-0.722	0.002	0.477	0.254-0.897	0.022

^aGoodness of fit test: Likelihood ratio (LR): Chi-squared test value, 27.90; P=0.000; Wald: Chi-squared test value, 28.11; P=0.000; score: Chi-squared test value, 31.00; P=0.000. HR, hazard ratio; 95% CI, 95% confidence interval. Values in bold font indicate statistically significant differences (P<0.05). KLF4, Krüppel like factor 4; pCCA, perihilar cholangiocarcinoma.

apoptotic FRH0201 cells in the shKLF4 group using Annexin V-PE staining. The silencing of KLF4 was shown to suppress FRH0201 cell apoptosis (control group, 12.45%; NC group, 12.52%; shKLF4 group, 7.05%; P<0.001; Fig. 3A), findings

that were in accordance with the results of the TUNEL assays (P<0.001; Fig. 3B). These findings were additionally supported by the changes in the levels of biomarker proteins associated with apoptosis. Western blot analysis demonstrated that the

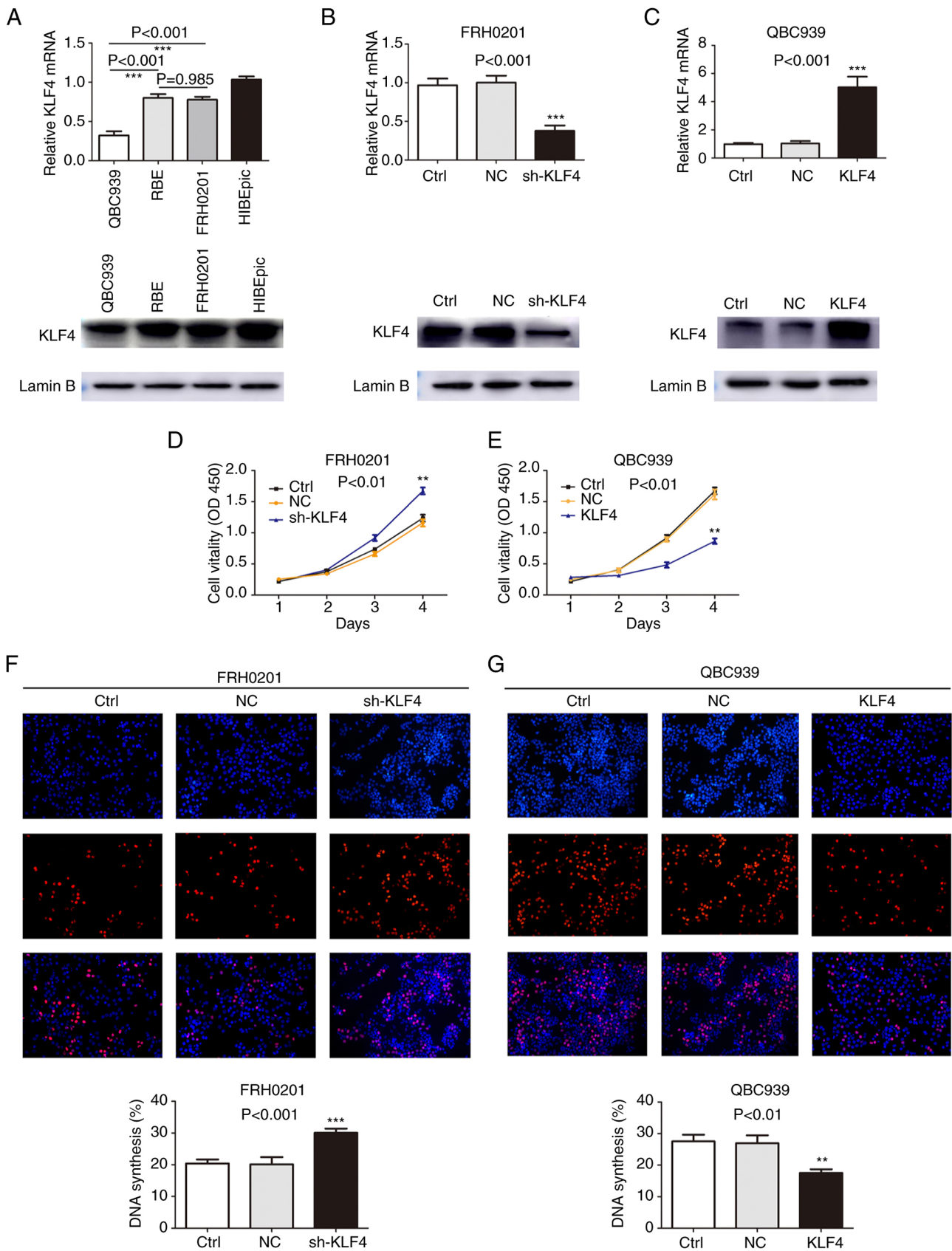


Figure 2. KLF4 suppresses the proliferation of pCCA cells. (A) KLF4 expression levels in the human pCCA cell lines, QBC939, RBE and FRH0201, and the human intrahepatic biliary epithelial cells (HIBEpIC) were detected using RT-qPCR and western blot analyses. Lamin B served as the loading control in the western blot analysis experiments. (B) Knockdown of KLF4 in FRH-0201 cells with lentivirus infection was verified using RT-qPCR and western blot analyses. (C) The efficiency of KLF4 overexpression using the designated plasmid was verified using RT-qPCR and western blot analyses. (D and F) CCK-8 and EdU assays were used to detect the proliferation of FRH0201 cells, wherein KLF4 was knocked down. (E and G) QBC939 cell proliferation was analyzed using CCK-8 and EdU assays following transfection with the KLF4 overexpression plasmid. **P<0.01 and ***P<0.001, vs. control group, without transfection. Ctrl, control; NC group, transfected with a non-coding shRNA; shKLF4 group, transfected with the KLF4-specific shRNA; KLF4 group, transfected with the KLF4-over-expression plasmid. KLF4, Krüppel-like factor 4; pCCA, perihilar cholangiocarcinoma; RT-qPCR, reverse transcription-quantitative PCR.

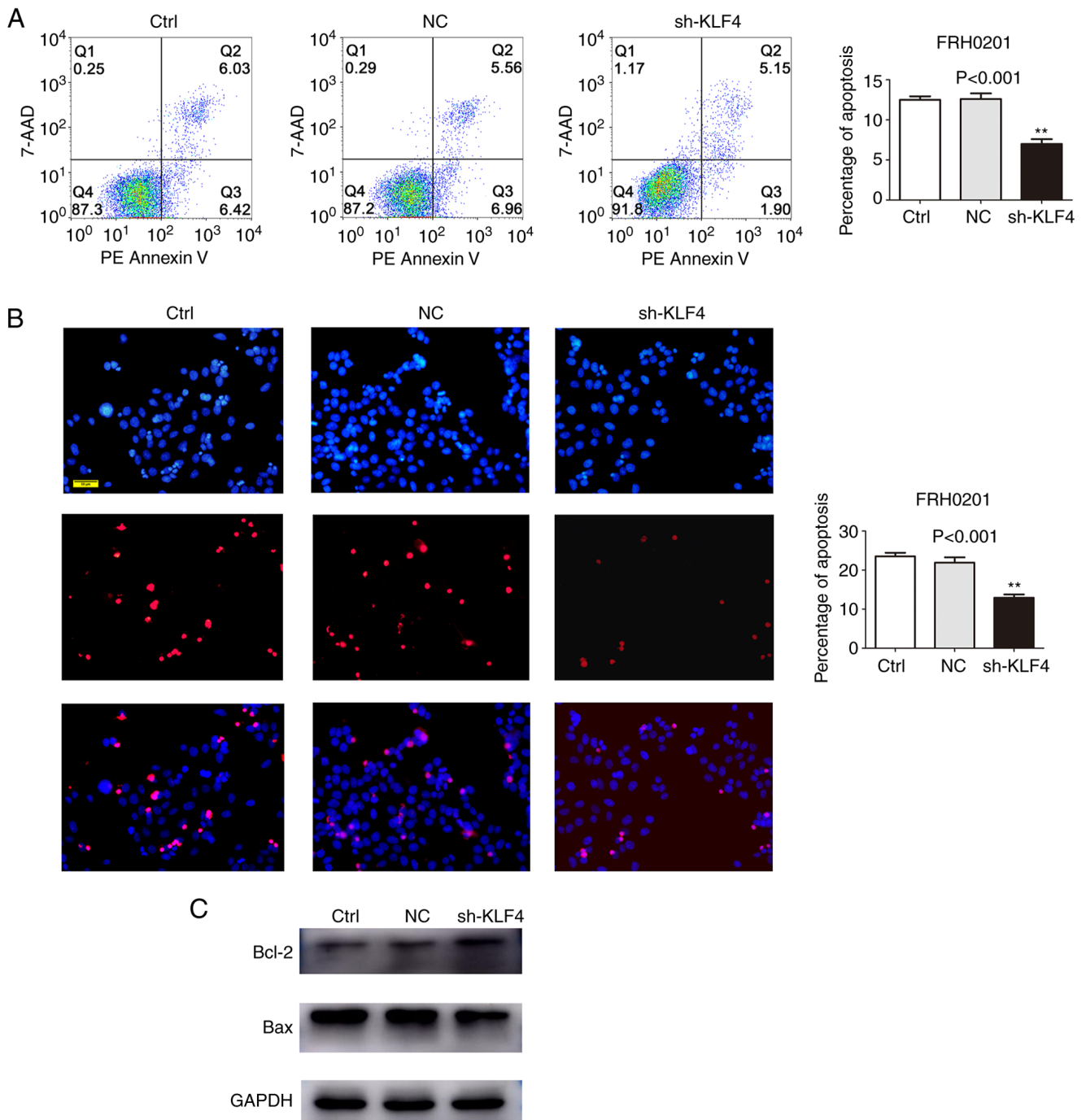


Figure 3. Knockdown of KLF4 expression suppresses the apoptosis of FRH0201 cells. (A) Flow cytometric analysis of apoptosis was performed to evaluate FRH0201 cell apoptosis following the knockdown of KLF4. (B) A TUNEL assay was performed to assess FRH0201 cell apoptosis following the knockdown of KLF4. Scale bar, 50 μ m. (C) Bcl-2 and Bax expression levels were measured using western blot analysis. ** $P < 0.01$, vs. control group, without transfection. Ctrl, control; NC group, transfected with a non-coding shRNA; shKLF4 group, transfected with the KLF4-specific shRNA; KLF4, Krüppel-like factor 4.

level of Bcl-2 was higher and the level of Bax was lower, in the shKLF4 group compared with the control and NC groups (Fig. 3C).

Inverse association between the expression levels of KLF4 and GDF15 in pCCA. By using the GEO2R online tool from the Gene Expression Omnibus (GEO), a total of 503 differentially expressed genes (DEGs) were identified (of which 195 were upregulated and 308 were downregulated DEGs) in the GSE26566 dataset, and 455 DEGs (27 upregulated and

428 downregulated) were found in the GSE89749 dataset, which were differentially expressed between tumor samples and adjacent normal tissues, as shown by the volcano plots in Fig. S1A and B (a threshold defined by a $\log_2FC \geq 1.5$ and $P < 0.05$). Further analysis of these DEGs using a Venn diagram (Fig. S1C) revealed that there were 61 overlapping DEGs (7 upregulated and 54 downregulated DEGs) comparing between the two datasets, as shown in Table SI.

The hTFtarget and TRRUST databases were further explored to obtain two KLF4 target datasets. A Venn diagram

was constructed to identify one gene at the intersection of two KLF4 target datasets and 61 overlapping DEGs, which was found to be GDF15 (Fig. S1D).

On the basis of the aforementioned bioinformatics analyses, it was hypothesized that GDF15 was a downstream target of KLF4. Therefore, the expression levels of KLF4 and GDF15 were further evaluated in the pCCA TMAs in order to confirm this association. As shown in Fig. 4A, the high expression of GDF15 mainly occurred in the tumor tissue samples with a low KLF4 expression, whereas the tumor tissue samples with a high expression of KLF4 had lower levels of GDF15. Spearman's correlation analysis of the IHC scores demonstrated the inverse association between KLF4 and GDF15 ($Rho = -0.1917$, $P = 0.0411$; Fig. 4B). This result was further confirmed by the Pearson's correlation analysis of the expression of KLF4 and GDF15 (data from RT-qPCR analysis of 20 pairs of fresh tumor tissues) ($r = -0.4836$, $P = 0.0308$; Fig. 4C).

Knockdown of KLF4 promotes the expression of GDF15 and phosphorylation of AKT. To further explore the direct correlation between KLF4 and GDF15, the effects of KLF4 on GDF15 expression in human pCCA FRH-0201 cells were examined. Furthermore, changes in the levels of AKT and p-AKT were also detected, since they are the downstream targets of GDF15 (26). These experiments revealed that the silencing of KLF4 led to a significant increase in the levels of GDF15 and p-AKT (Fig. 4D). In the cells in which the expression of GDF15 was interfered with, the promoting effects of the silencing of KLF4 on p-AKT were found to be attenuated (Fig. 4E). Taken together, these results suggested that KLF4 adjusted and regulated the AKT signaling pathway by negatively regulating GDF15, whereas the overexpression of GDF15 mediated by a deficiency of KLF4 may contribute to pCCA tumor carcinogenesis and development.

Knockdown of KLF4 expression promotes tumor growth in vivo. As shown in Fig. 5A and C, the knockdown of KLF4 expression led to a marked promotion of tumor growth compared with NC transfection in the animal models. In addition, the average tumor weight was lower in the NC group compared with the shKLF4 group (242.2 ± 35.94 vs. 548.60 ± 48.61 mg; Fig. 5B and Table SII). As shown by the results of western blot analysis and IHC, the knockdown of KLF4 led to an increase in the expression of GDF15 in the *in vivo* experiment (Fig. 5D and E). Furthermore, the level of p-AKT pertaining to the *in vivo* experiments was also measured using western blot analysis; the results revealed that the level of p-AKT was found to have increased, along with the augmentation of the GDF15 signal in the shKLF4 group (Fig. 5D). These results were in accordance with those obtained in the *in vitro* experiments, further confirming that the knockdown of KLF4 expression promoted the progression of pCCA.

Discussion

Despite the recent developments in early diagnosis and individual therapy, CCA still remains a highly lethal tumor (31). Moreover, pCCA is the most common subtype of CCA, which is associated with the worst prognosis (32). This is partly due to the lack of novel biomarkers or molecular profiles and targeted

drugs for pCCA. Therefore, there is an urgent need to unravel the underlying molecular mechanisms of the oncogenesis and progression of pCCA.

In the present study, the expression levels and potential roles of KLF4 and GDF15 in human pCCA were determined. It was confirmed that the expression level of KLF4 was decreased in pCCA tumor tissues and cell lines. Further analysis of the association between the clinicopathological characteristics of patients with pCCA and the expression levels of KLF4 using TMAs revealed that the absence of KLF4 was closely associated with a poor histological grade and a large tumor size, also predicting a poor OS. Multivariate analysis indicated that KLF4 was an independent favorable prognosis factor in patients with pCCA. In addition, the cell proliferative ability was reinforced, and cell apoptosis was suppressed, when KLF4 was knocked down using shRNA. Finally, cell proliferation was shown to be suppressed when KLF4 was overexpressed.

KLF4 is a critical member of the KLF family. It fulfills crucial roles in tumor emergence, progression, invasion and metastasis (9,33). KLF4 was originally shown to be a tumor suppressor (12,27); however, numerous studies have demonstrated that it encodes a transcription factor that is associated with both tumor suppression and oncogenesis (11,14,34) {Rowland, 2005 #296}. Several previously published studies have demonstrated that KLF4 expression is decreased in tumor types, such as gastrointestinal cancers (11), colorectal cancer (12), lung cancer (35) and so on (13,27), and KLF4 overexpression is a predictor of an improved prognosis (35,36). In accordance with these findings, the results of the present study demonstrated that KLF4 expression was decreased in pCCA compared with adjacent tissues. However, tentative evidence has indicated that KLF4 may function as an oncogene in primary breast cancer, prostate cancer and skin cancer (14,15,37). The role of KLF4 in terms of regulating tumors is dependent on the different cellular contexts, the expression patterns of other genes, and so on (34,38,39). KLF4 can execute its tumor suppressive functions directly or indirectly by regulating the cell cycle, as an anti-apoptosis molecule, and via the Wnt, Notch and TGF- β signaling pathways, and so on (8,9,40,41). GDF15 is usually expressed abundantly under conditions of stress, inflammation, diabetes, cardiovascular disorder, cancer and so on (42). However, the mechanisms underlying its activation and regulation remains poorly understood. It has been shown that AKT signaling is associated with cell proliferation and survival (anti-apoptosis) (43). A disruption in the balance between cell proliferation and survival leads to the development and progression of cancer (26,30). Moreover, it has been confirmed that GDF15 is able to activate AKT when the balance between cell proliferation and survival is disrupted (26). In the present study, the expression of GDF15 in TMAs was further investigated. The results obtained demonstrated that the pCCA specimens in the TMA analysis, which lost their KLF4 expression, had a high expression of GDF15. Spearman's correlation analysis confirmed the negative association between them. This association was also confirmed using RT-qPCR analysis. Moreover, bioinformatics analyses revealed that GDF15 was identified as the only DEG that targeted KLF4 in pCCA. Therefore, it can be hypothesized that GDF15 is a key downstream target of KLF4 that

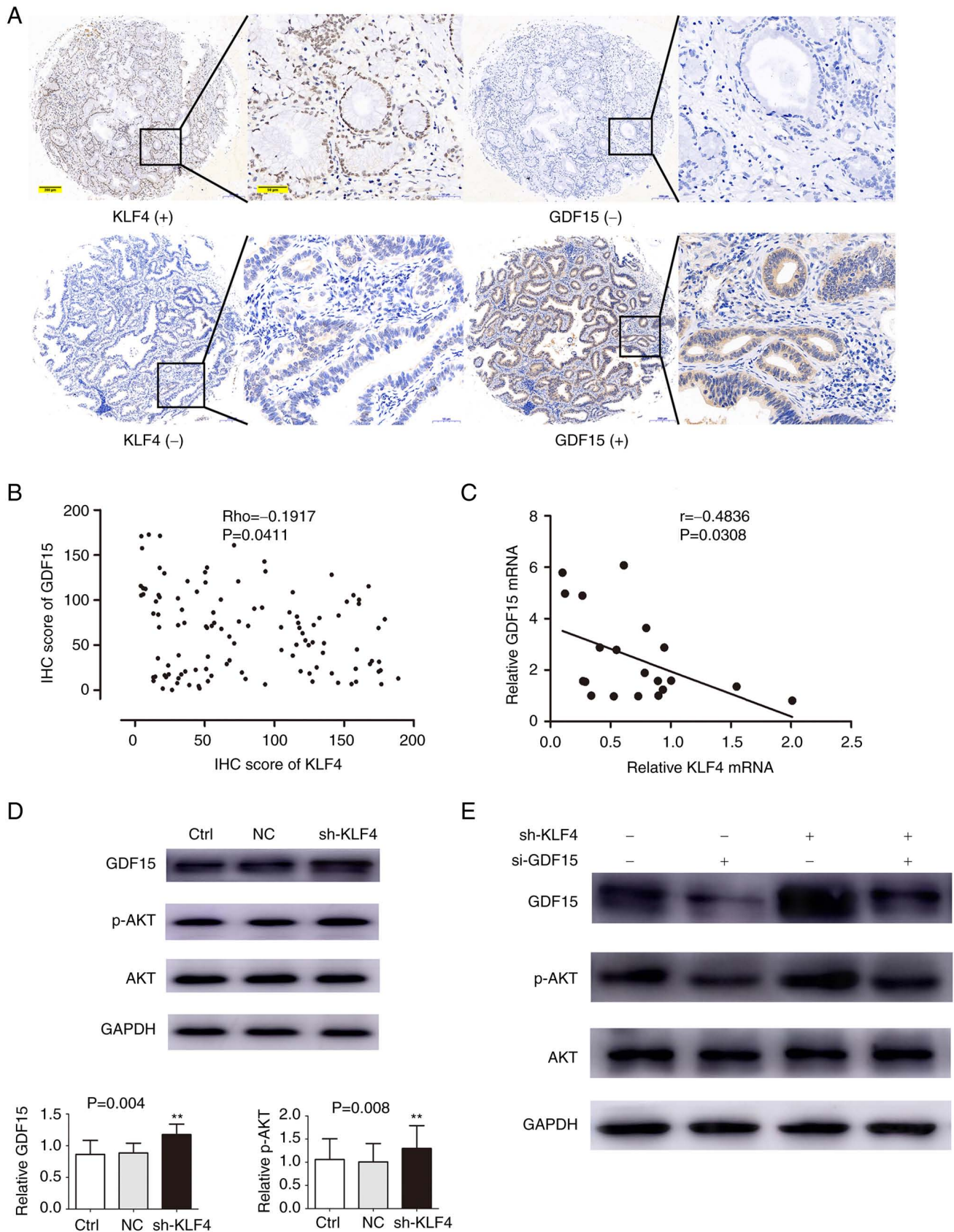


Figure 4. GDF15 expression is negatively associated with KLF4 expression in human pCCA tissue. KLF4 suppresses the protein expression of GDF15, thereby regulating the AKT pathway. (A) GDF15 expression was low in KLF4-positive tissue samples, and high in KLF4-negative tissue samples. Scale bars: Left panels, 200 μ m; right panels, 50 μ m. (B) Correlation of IHC scores for KLF4 and GDF15 in human pCCA tissues ($r = -0.2124$, $P = 0.0233$). (C) Correlation of mRNA expression for KLF4 and GDF15 in human pCCA tissues ($r = -0.4836$, $P = 0.0308$). (D) Variations in the levels of GDF15 and p-AKT were examined using western blot analysis following the knockdown of KLF4. (E) Western blot analysis revealed that the increase in p-AKT expression due to knockdown of KLF4 could be circumvented by si-GDF15. ** $P < 0.01$, vs. control group, without transfection. Ctrl group, control group, without transfection; NC group, transfected with a non-coding shRNA; shKLF4 group, transfected with the KLF4-specific shRNA; si-GDF15 group, siRNA targeting GDF15; KLF4, Krüppel-like factor 4; pCCA, perihilar cholangiocarcinoma; GDF15, growth/differentiation factor 15; KLF4, Krüppel-like factor 4.

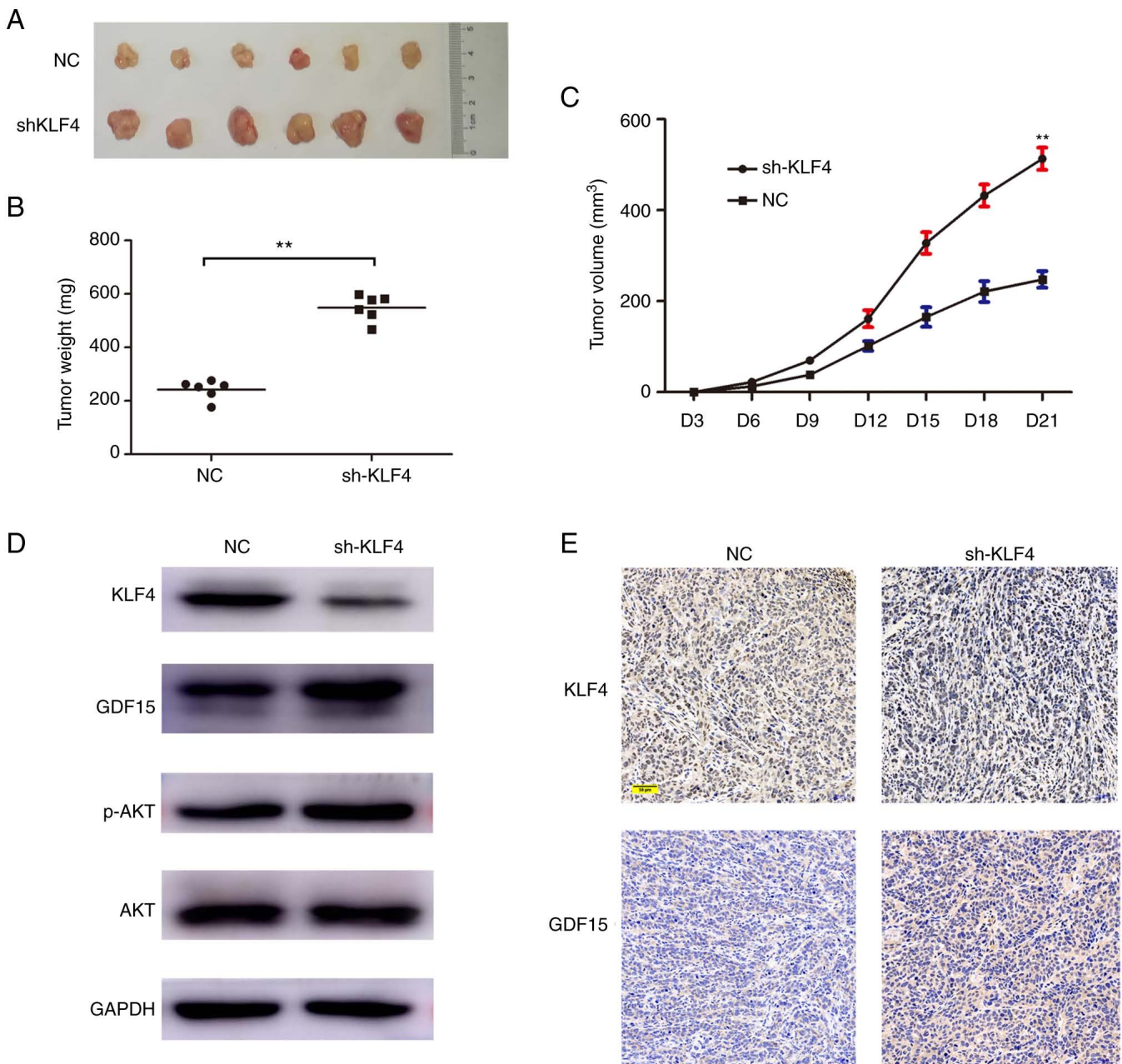


Figure 5. KLF4 inhibits the growth of HCCA xenograft tumors. (A) Stable shKLF4 cells and control cells (transfected with empty vector) were injected subcutaneously into the right flanks of BALB/c nude mice. At 3 weeks after implantation, xenograft tumors were observed. (B) Tumor volumes were measured every 3 days until the mice were euthanized on day 21. (C) Tumor weights were measured on day 21. (D) The expression levels of KLF4, GDF15, AKT and p-AKT in tumors were measured using western blot analysis. (E) Immunohistochemical staining revealed the association between KLF4 and GDF15 in xenograft tumors. Scale bar, 50 μ m. **P<0.01, vs. control. Ctrl, control group without transfection; NC group, transfected with a non-coding shRNA; shKLF4 group, transfected with the KLF4 specific shRNA; KLF4, Krüppel like factor 4; pCCA, perihilar cholangiocarcinoma; GDF15, growth/differentiation factor 15; p, phosphorylated.

functions as a transcription factor in pCCA, as demonstrated herein. In the present study, further experiments indicated that the silencing KLF4 increased both the expression of GDF15 and the phosphorylation of AKT *in vitro*. Moreover, the knockdown of GDF15 attenuated the suppressive effects of KLF4 on the AKT pathway. These findings indicated that KLF4, as a transcription factor, executes its tumor-suppressive role by regulating the GDF15/AKT signaling pathway.

In conclusion, the present study demonstrated that the loss of KLF4 in human pCCA results in the overexpression of GDF15, thereby leading to the active phosphorylation of

AKT and subsequent tumor progression. The findings of the present study not only provide a novel molecular mechanism of pCCA tumor progression, but the KLF4/GDF15/AKT signaling pathway has also been identified as a potential novel molecular target for controlling pCCA tumor development. KLF4 itself may prove to be a useful biomarker for predicting the prognosis of patients with pCCA.

Acknowledgements

Not applicable.

Funding

No funding was received.

Availability of data and materials

The datasets used and/or analyzed during the current study are available from the corresponding author on reasonable request.

Authors' contributions

XZ, CL and HZ were involved in the conception and design of the study. XZ and CL performed the research. XZ and WW were involved data analysis and interpretation. All authors were involved in the writing of the manuscript. XZ, CL and HZ confirm the authenticity of all the raw data. All authors have read and approved the final manuscript.

Ethics approval and consent to participate

For the use of human samples, the present study was approved by the Medical Ethics Committee of Linyi People's Hospital (approval no. YX200626). Written informed consent was obtained from all patients. All animal experiments were approved by the Medical Ethics Committee of Linyi People's Hospital. They were executed in accordance with the guidelines for the use and care of laboratory animals provided by Linyi People's Hospital.

Patient consent for publication

Not applicable.

Competing interests

The authors declare that they have no competing interests.

References

- Brindley PJ, Bachini M, Ilyas SI, Khan SA, Loukas A, Sirica AE, Teh BT, Wongkham S and Gores GJ: Cholangiocarcinoma. *Nat Rev Dis Primers* 7: 65, 2021.
- Banales JM, Marin JGG, Lamarca A, Rodrigues PM, Khan SA, Roberts LR, Cardinale V, Carpino G, Andersen JB, Braconi C, *et al*: Cholangiocarcinoma 2020: The next horizon in mechanisms and management. *Nat Rev Gastroenterol Hepatol* 17: 557-588, 2020.
- Krasinskas AM: Cholangiocarcinoma. *Surg Pathol Clin* 11: 403-429, 2018.
- Rizvi S and Gores GJ: Pathogenesis, diagnosis, and management of cholangiocarcinoma. *Gastroenterology* 145: 1215-1229, 2013.
- Khan AS and Dageforde LA: Cholangiocarcinoma. *Surg Clin North Am* 99: 315-335, 2019.
- Deoliveira ML, Cunningham SC, Cameron JL, Kamangar F, Winter JM, Lillemoie KD, Choti MA, Yeo CJ and Schulick RD: Cholangiocarcinoma: Thirty-one-year experience with 564 patients at a single institution. *Ann Surg* 245: 755-762, 2007.
- Groot Koerkamp B, Wiggers JK, Gonen M, Doussot A, Allen PJ, Besselink MG, Blumgart LH, Busch OR, D'angelica MI, DeMatteo RP, *et al*: Survival after resection of perihilar cholangiocarcinoma-development and external validation of a prognostic nomogram. *Ann Oncol* 27: 753, 2016.
- Ghaleb AM and Yang VW: Krüppel-like factor 4 (KLF4): What we currently know. *Gene* 611: 27-37, 2017.
- Luo X, Zhang Y, Meng Y, Ji M and Wang Y: Prognostic significance of KLF4 in solid tumours: An updated meta-analysis. *BMC Cancer* 22: 181, 2022.
- Wang N, Liu ZH, Ding F, Wang XQ, Zhou CN and Wu M: Down-regulation of gut-enriched Krüppel-like factor expression in esophageal cancer. *World J Gastroenterol* 8: 966-970, 2002.
- Wei D, Kanai M, Huang S and Xie K: Emerging role of KLF4 in human gastrointestinal cancer. *Carcinogenesis* 27: 23-31, 2006.
- Zhao W, Hisamuddin IM, Nandan MO, Babbins BA, Lamb NE and Yang VW: Identification of Krüppel-like factor 4 as a potential tumor suppressor gene in colorectal cancer. *Oncogene* 23: 395-402, 2004.
- Ohnishi S, Ohnami S, Laub F, Aoki K, Suzuki K, Kanai Y, Haga K, Asaka M, Ramirez F and Yoshida T: Downregulation and growth inhibitory effect of epithelial-type Krüppel-like transcription factor KLF4, but not KLF5, in bladder cancer. *Biochem Biophys Res Commun* 308: 251-256, 2003.
- Pandya AY, Talley LI, Frost AR, Fitzgerald TJ, Trivedi V, Chakravarthy M, Chhieng DC, Grizzle WE, Engler JA, Krontiras H, *et al*: Nuclear localization of KLF4 is associated with an aggressive phenotype in early-stage breast cancer. *Clin Cancer Res* 10: 2709-2719, 2004.
- Jiang Z, Zhang Y, Chen X, Wu P and Chen D: Long non-coding RNA LINC00673 silencing inhibits proliferation and drug resistance of prostate cancer cells via decreasing KLF4 promoter methylation. *J Cell Mol Med* 24: 1878-1892, 2020.
- Zhao C, Li Y, Qiu W, He F, Zhang W, Zhao D, Zhang Z, Zhang E, Ma P, Liu Y, *et al*: C5a induces A549 cell proliferation of non-small cell lung cancer via GDF15 gene activation mediated by GCN5-dependent KLF5 acetylation. *Oncogene* 37: 4821-4837, 2018.
- Li S, Ma YM, Zheng PS and Zhang P: GDF15 promotes the proliferation of cervical cancer cells by phosphorylating AKT1 and Erk1/2 through the receptor ErbB2. *J Exp Clin Cancer Res* 37: 80, 2018.
- Xu Q, Xu HX, Li JP, Wang S, Fu Z, Jia J, Wang L, Zhu ZF, Lu R and Yao Z: Growth differentiation factor 15 induces growth and metastasis of human liver cancer stem-like cells via AKT/GSK-3 β / β -catenin signaling. *Oncotarget* 8: 16972-16987, 2017.
- Jin Y, Jung SN, Lim MA, Oh C, Piao Y, Kim HJ, Liu L, Kang YE, Chang JW, Won HR, *et al*: Transcriptional regulation of GDF15 by EGR1 promotes head and neck cancer progression through a positive feedback loop. *Int J Mol Sci* 22: 11151, 2021.
- Dong G, Huang X, Jiang S, Ni L, Ma L, Zhu C and Chen S: SCAP mediated GDF15-induced invasion and EMT of esophageal cancer. *Front Oncol* 10: 564785, 2020.
- Joshi JP, Brown NE, Griner SE and Nahta R: Growth differentiation factor 15 (GDF15)-mediated HER2 phosphorylation reduces trastuzumab sensitivity of HER2-overexpressing breast cancer cells. *Biochem Pharmacol* 82: 1090-1099, 2011.
- Huang M, Narita S, Koizumi A, Nara T, Numakura K, Satoh S, Nanjo H and Habuchi T: Macrophage inhibitory cytokine-1 induced by a high-fat diet promotes prostate cancer progression by stimulating tumor-promoting cytokine production from tumor stromal cells. *Cancer Commun (Lond)* 41: 389-403, 2021.
- Yan Y, Yue X, Yang S, Zhao Z, Wu P and Liu H: The expression of growth differentiation factor 15 in gallbladder carcinoma. *J BUON* 26: 218-228, 2021.
- Li C, Wang J, Kong J, Tang J, Wu Y, Xu E, Zhang H and Lai M: GDF15 promotes EMT and metastasis in colorectal cancer. *Oncotarget* 7: 860-872, 2016.
- Wang X, Baek SJ and Eling TE: The diverse roles of nonsteroidal anti-inflammatory drug activated gene (NAG-1/GDF15) in cancer. *Biochem Pharmacol* 85: 597-606, 2013.
- Fang L, Li F and Gu C: GDF-15: A multifunctional modulator and potential therapeutic target in cancer. *Curr Pharm Des* 25: 654-662, 2019.
- Yang Y, Goldstein BG, Chao HH and Katz JP: KLF4 and KLF5 regulate proliferation, apoptosis and invasion in esophageal cancer cells. *Cancer Biol Ther* 4: 1216-1221, 2005.
- Li JC, Chen QH, Jian R, Zhou JR, Xu Y, Lu F, Li JQ and Zhang H: The partial role of KLF4 and KLF5 in gastrointestinal tumors. *Gastroenterol Res Pract* 2021: 2425356, 2021.
- Livak KJ and Schmittgen TD: Analysis of relative gene expression data using real-time quantitative PCR and the 2(-Delta Delta C(T)) method. *Methods* 25: 402-408, 2001.
- Evan GI and Vousden KH: Proliferation, cell cycle and apoptosis in cancer. *Nature* 411: 342-348, 2001.
- Razumilava N and Gores GJ: Cholangiocarcinoma. *Lancet* 383: 2168-2179, 2014.
- Zhang XM, Liu ZL, Qiu B, Xu YF, Pan C and Zhang ZL: Downregulation of EVI1 expression inhibits cell proliferation and induces apoptosis in hilar cholangiocarcinoma via the PTEN/AKT signalling pathway. *J Cancer* 11: 1412-1423, 2020.

33. Guo K, Cui J, Quan M, Xie D, Jia Z, Wei D, Wang L, Gao Y, Ma Q and Xie K: The novel KLF4/MSI2 signaling pathway regulates growth and metastasis of pancreatic cancer. *Clin Cancer Res* 23: 687-696, 2017.
34. Rowland BD, Bernards R and Peeper DS: The KLF4 tumour suppressor is a transcriptional repressor of p53 that acts as a context-dependent oncogene. *Nat Cell Biol* 7: 1074-1082, 2005.
35. Hu W, Hofstetter WL, Li H, Zhou Y, He Y, Pataer A, Wang L, Xie K, Swisher SG and Fang B: Putative tumor-suppressive function of Kruppel-like factor 4 in primary lung carcinoma. *Clin Cancer Res* 15: 5688-5695, 2009.
36. Patel NV, Ghaleb AM, Nandan MO and Yang VW: Expression of the tumor suppressor Kruppel-like factor 4 as a prognostic predictor for colon cancer. *Cancer Epidemiol Biomarkers Prev* 19: 2631-2638, 2010.
37. Chen YJ, Wu CY, Chang CC, Ma CJ, Li MC and Chen CM: Nuclear Kruppel-like factor 4 expression is associated with human skin squamous cell carcinoma progression and metastasis. *Cancer Biol Ther* 7: 777-782, 2008.
38. Hu W, Jia Y, Xiao X, Lv K, Chen Y, Wang L, Luo X, Liu T, Li W, Li Y, *et al*: KLF4 downregulates hTERT expression and telomerase activity to inhibit lung carcinoma growth. *Oncotarget* 7: 52870-52887, 2016.
39. Rowland BD and Peeper DS: KLF4, p21 and context-dependent opposing forces in cancer. *Nat Rev Cancer* 6: 11-23, 2006.
40. Ghaleb AM, McConnell BB, Kaestner KH and Yang VW: Altered intestinal epithelial homeostasis in mice with intestine-specific deletion of the Kruppel-like factor 4 gene. *Dev Biol* 349: 310-320, 2011.
41. Cui J, Shi M, Quan M and Xie K: Regulation of EMT by KLF4 in gastrointestinal cancer. *Curr Cancer Drug Targets* 13: 986-999, 2013.
42. Modi A, Purohit P, Roy D, Vishnoi JR, Pareek P, Elhence P, Singh P, Sharma S, Sharma P and Misra S: FOXM1 mediates GDF-15 dependent stemness and intrinsic drug resistance in breast cancer. *Mol Biol Rep* 49: 2877-2888, 2022.
43. Vivanco I and Sawyers CL: The phosphatidylinositol 3-Kinase AKT pathway in human cancer. *Nat Rev Cancer* 2: 489-501, 2002.



Copyright © 2023 Zhang et al. This work is licensed under a Creative Commons Attribution-NonCommercial-NoDerivatives 4.0 International (CC BY-NC-ND 4.0) License.